The black hole mass vs bulge velocity dispersion relation.

Fernando Becerra

Harvard-Smithsonian Center for Astrophysics, Harvard University, Cambridge, MA 02138

Astronomy 202a Term Paper

fbecerra@cfa.harvard.edu

1. Introduction

Black holes (BHs) are known to be a key ingredient in the formation and evolution of galaxies. Early studies from the 1990s suggest a correlation between black hole mass ($M_{\rm BH}$) and the luminosity ($L_{\rm bulge}$) of the host galaxy (Kormendy & Richstone 1995, Magorrian et al. 1998). More recent studies have extended the correlation between small scales properties of the central black hole and large scale properties of the galaxy, and have proposed a $M_{\rm BH}$-σ (Ferrarese & Merritt 2000, Gebhardt et al. 2000) and a $M_{\rm BH}$-$M_{\rm bulge}$ (Marconi & Hunt 2003) correlations. Among these, the one that highlights by its low scatter is the $M_{\rm BH}$-σ relation, quoted to be a scatter comparable to measurement errors. The most general form of this relation is given by

$$\log\left(M_{\rm BH}/M_{\odot}\right) = \alpha + \beta \log\left(\sigma/\sigma_0\right) \tag{1}$$

where the black hole mass has been normalized to solar masses, and the velocity dispersion has been normalized to a value σ_0, which is usually taken to be 220 km s^{-1}. The parameters α and β correspond to the zero points and the slope of the fit, respectively. Since the seminal works of Ferrarese & Merritt (2000) and Gebhardt et al. (2000), many attempts of measuring the slope has been carried out (Merritt & Ferrarese 2001, Ferrarese 2002, Tremaine et al. 2002, Ferrarese & Ford 2005, Gültekin et al. 2009, Kormendy & Ho 2013), but a consensus in the value of β has not been reached yet.

As new observational techniques are developed and higher-resolution data becomes available, this relation have suffered some modifications since their initial measurement. For instance, at the beginning it was thought that this relation held for every galaxy containing a black hole at its center. But recent studies have shown that this is not true, and that the relation holds only for some galaxies. In particular, Kormendy & Ho (2013) argue that pseudobulges and disk galaxies do not follow the $M_{\rm BH} - \sigma$ relation, and that this is only valid for ellipticals and classical bulges.

The distinction between bulges and pseudobulges is purely based on observational constraints. Despite the fact that the criteria is not well-defined, we can distinguish common properties among bulges and pseudobulges. For example, in general, bulges have morphology very similar to ellipticals, and they may even follow the same relations of the fundamental plane for those galaxies. In contrast, pseudobulges are more disk-like, even presenting spiral structures in some cases. Their

origin is another point of differences between those objects. Bulges are believed to form as a consequence of major mergers, while pseudobulges might form from secular evolution internal to isolated disk galaxies. Kormendy & Ho (2013) refined the selection criteria to discriminate between them. Their main points are:

- Pseudobulges often have disky morphology while classical bulges are much rounder than their disks unless the galaxy is almost face-on.
- Although the processes that determine Sérsic indices are not completely understood, most pseudobulges have Sersic (1968) indices $n < 2$; almost all classical bulges have n ≥ 2. However, it is worth mentioning that some pseudobulges do have Sérsic indices as big as 4.
- Pseudobulges are slightly more rotation-dominated than classical bulges in the $V_{max}/\sigma - \epsilon$ diagram; e.g., $(V_{max}/\sigma)^* > 1$. In two-dimensional velocity fields, pseudobulges generally appear as distinct, rapidly rotating, and dynamically cold, central disk-like components.
- Many pseudobulges are low-σ outliers in the Faber-Jackson correlation (Faber & Jackson 1976) between (pseudo)bulge luminosity and velocity dispersion, or σ decreases from the disk into the pseudobulge.
- Classical bulges fit the fundamental plane correlations for elliptical galaxies. Some pseudobulges do, too, and then these correlations are not helpful for classification. But extreme pseudobulges have larger effective radii r_e and fainter effective surface brightnesses μ_e at r_e.
- Small bulge-to-total luminosity ratios do not guarantee that a bulge is pseudo, but B/T $\gtrsim$ 0.5 implies that the bulge is classical.

A particular property of galaxies containing a bulge or pseudobulge is that, it is believed that a very massive central object resides at the center of those galaxies. Those massive objects are known as black holes. In particular, if the mass of a BH lies in the range between $10^6 M_\odot$ and $10^9 M_\odot$, they are usually referred as Supermassive Black Holes (SMBHs). Due to their masses, these objects are able to accrete huge amount of gas and radiate energy. This phenomena is commonly observed in Seyfert galaxies, radio galaxies, and quasars and it is usually called Active Galactic Nuclei (AGN).

The maximum luminosity at which these objects can emit, can be deduced assuming equilibrium between the force due to radiative pressure, $F_{\rm rad}$, and the force due to gravity, $F_{\rm g}$. Expressing the radiative force as $F_{\rm rad} = P_{\rm rad}\sigma_{\rm T} = L\sigma_T/(4\pi cr)$, where $\sigma_{\rm T}$ is the Thomson cross-section for electron scattering, and the gravitational force as $F_{\rm g} = GM_{\rm BH}m_{\rm p}/r^2$, we can obtain an expression for the luminosity:

$$L_{\rm Edd} = \frac{4\pi G c m_{\rm p}}{\sigma_{\rm T}} M_{\rm BH} \approx 1.26 \times 10^{38} \left(\frac{M_{\rm BH}}{M_\odot}\right) \text{ergs s}^{-1} \tag{2}$$

which is referred as "Eddington luminosity" or "Eddington limit". This limit can be also be related to the accretion rate of the BH. Considering that the energy that can be extracted from a mass

$M_{\rm BH}$ is a fraction of its rest mass, i.e. $E = \eta M_{\rm BH} c^2$ with η an efficiency factor, we can rewrite the luminosity as the derivative of the energy with respect to time, as:

$$L = \frac{dE}{dt} = \eta \dot{M}_{\rm BH} c^2 \tag{3}$$

where $\dot{M}_{\rm BH} = dM_{\rm BH}/dt$ is the mass accretion rate.

We can also define a "boundary" for these objects, defined as the radius at which gravitational time dilation goes to infinity and lengths are contracted to zero. This radius is known as the Schwarzschild radius, and can be calculated setting the speed of light as the escape velocity:

$$R_{\rm Sch} = \frac{2GM_{\rm BH}}{c^2} \tag{4}$$

In the case of supermassive black holes we can define a "sphere of influence", defined as the region of space where the gravitational potential of the SMBH dominates over that of the surrounding gas and stars. The expression for the radius of influence is given by

$$R_{\rm infl} \equiv \frac{GM_{\rm BH}}{\sigma^2} \approx 11.2 \left(\frac{M_{\rm BH}}{10^8 M_\odot}\right) \left(\frac{\sigma}{200 \text{ km s}^{-1}}\right)^{-2} \text{pc} \tag{5}$$

where σ is the velocity dispersion of the surrounding material. For typical black holes masses and velocity dispersions, the radius of influence has a value between 1 and 100 pc. Inside this radius, motions of stars and gas are dominated by a combination between the gravitational influence of the black hole, stars, dust, gas, and dark matter, which results in a predominantly Keplerian motion. Beyond this radius, the gravitational dominance of the SMBH quickly vanishes.

The order of this paper is as follow. In Section 2 we give a brief review of the main techniques used to estimate black hole masses. In Section 3 we analyze in detail the $M_{\rm BH} - \sigma$ relation, discussing how it has changed since the first measurements, and putting emphasis in the main sources of errors. We then discuss other scaling relations in Section 4, such as de $M_{\rm BH} - L_{\rm bulge}$ and the $M_{\rm BH} - M_{\rm bulge}$ relations. We finally conclude in Section 5.

2. Measuring black hole masses

Measuring the mass of the black hole has been a challenging issue since the first confirmation of the existence of such objects. It was not until the launch of the Hubble Space Telescope (HST) that black hole mass measurements increased drastically. Since then, many techniques to estimate the mass of a black hole have been developed. Among them, we find stellar dynamics, gas dynamics, maser dynamics and reverberation mapping. Most them rely on the basic principle that the black hole dominates the gravitational potential in its surroundings, and hence the dynamics of the material inside the radius of influence will be strongly influenced by the mass of the central object.

The most commonly used method nowadays, referred as stellar dynamics, uses measurements of the motions of stars close to the black hole. In particular, the three-integral method is currently the most reliable way to estimate BH masses. Besides stellar dynamics, we can also use the motion of gas as an estimation of the mass of the central object. Analogously, we can estimate the mass of the black hole by studying the dynamics of water megamasers in its vicinity. In the case of black holes in AGNs, the most popular technique is known as reverberation mapping. The latter technique allows to measure black holes of smaller masses known as intermediate massive black holes (IMBHs).

2.1. Stellar dynamics

Estimation of BH masses using this method are based on two equations. The first one corresponds to the Collissionless Boltzmann Equation (CBE), which relates the distribution function (f), the velocity field ($\vec{v}$) and the gravitational potential ($\Phi(\vec{x},t)$) of a stellar system through the formula:

$$\frac{\partial f}{\partial t} + \vec{v}\cdot\vec{\nabla} f - \vec{\nabla}\Phi(\vec{x},t)\cdot\frac{\partial f}{\partial \vec{v}} = 0 \tag{6}$$

In addition, we also need an equation relating the gravitational potential with the total mass distribution ($\rho(\vec{x},t)$), the so-called Poisson equation:

$$\nabla^2\Phi(\vec{x},t) = 4\pi G\rho(\vec{x},t) \tag{7}$$

From these equations, a first attempt would be to derive a distribution function from observational data. In particular, measuring the stellar mass density, the six components of the streaming velocity, and velocity dispersion would allow us to find an expression for f. Once the distribution function is known, we can replace its value in the CBE and derive the gravitational potential. The next step then is to use the Poisson equation, with which we can calculate the total mass density distribution given the gravitational potential. If the stellar mass density is known, then we can finally estimate the mass of the supermassive black hole. Unfortunately, obtaining stellar mass densities and velocity tensors from observations is very challenging and not always possible. Hence, to solve this pair of equations we have to come up with assumptions that will allow us to simplify the problem.

One common approach to overcome this difficulty is to assume anisotropy in the velocity. In such a case the distribution function must depend on at least two integrals of motion. In the simplest case, those integrals will be the total energy E and the vertical component of the angular momentum L_z, so the distribution function takes the form $f = f(E, L_z)$. The advantage of this simplification is that now we are able to write the distribution function in terms of two quantities that are easily derivable from observations. In particular, measurements of the mass density and the

tangential component of the streaming motion v_θ are enough to predict the distribution function. Unluckily, anisotropy in the velocity is not always a good assumption, and improvements to this method are needed.

A refinement to two-integrals methods are three-integrals methods. Their basic assumption is that the distribution function depends on a third integral of motion besides the energy and angular momentum. Unfortunately, the third integral does not have an analytical expression as the first two integrals. To overcome this limitation, the three-integrals method follow a completely different approach. Based on Schwarszchild's orbit superposition method to model galaxies, we start assuming a central back hole mass and a stellar population for the system. Given that, we can generate all the possible orbits for stars in the system as a function of energy and angular momentum, and integrated long enough to include information about time-averaged densities, velocities, and velocity dispersion of the stars. The next step is to compare these predictions to observations, and explore the free parameters to fit the data. The best fit will give us the final estimation of $M_{\rm BH}$. One of the disadvantages of this method is the lack of uniqueness in the answer, where different assumptions might produce the same predictions. Even though this drawback, this method gives very accurate estimates of the BH mass. Further improvements can be done to the three-integrals method, for instance Kormendy & Ho (2013) suggested that the gravitational effect of dark matter should be included in the models.

2.1.1. The special case of the Milky Way

Measurement of the mass of the black hole at the center of our Galaxy also uses stellar dynamics, based on spectroscopy of gas or stellar subpopulations. Given the distance from the solar system to the center of the Milky Way, we are able to completely resolve the inner regions of the Galaxy. This implies that we are able to follow the orbital motions of the stars in the cluster close to the black hole.

Observations have measured trajectories of those stars for over 40 stars. Two of them are particularly interesting because of their short orbital period. These objects constitute a very powerful tool since they can be observed during a whole orbit around the central BH in a human timescale. Figure 1 panel (a) shows orbits for 20 stars in the neighborhood of the center of our Galaxy. Highlighted in red is the orbit of the S2 star and a zoomed-in version of it is shown in panel (b). Its period has been measured to be 15.8 years and its orbit is almost closed, which tells us that almost all of the mass is located at its pericenter (shown in green in panel (b)). Measuring velocities (panel (c)), and assuming a Keplerian fit for the data we can easily estimate the mass of the black hole at that location. Recent studies have refined the mass of Sgr A* converging to a value $M_{\rm BH} = 4.30 \pm 0.20({\rm stat}) \pm 0.30({\rm sys}) \times 10^6 M_\odot$ (Genzel et al. 2010). Because of the very high resolution achieved in this region, this is by far the most accurate black hole mass estimation we have.

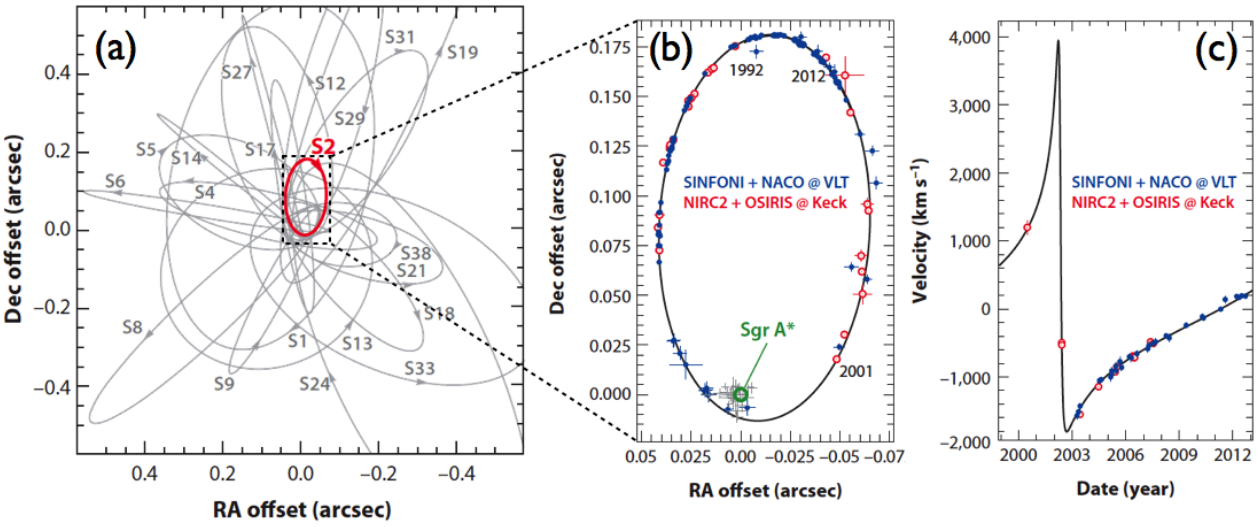

Fig. 1.— Measuring proper motion of stars in the center of the Milky Way. Panel (a) shows the orbit for almost 20 stars in the vicinity of the central black hole. Panel (b) shows a the orbit of the S2 star as measured from 1992 to 2012. Blue and red dots are observations, while in green it is shown the pericenter of the orbit, which coincides with the location of Sgr A*. Panel (c) shows the velocity curve for the same star. Adapted from Kormendy & Ho (2013)

2.2. Gas dynamics

Measuring black hole masses using gas dynamics is based in observing nebular emission lines from the central gas/dust disk in the galaxies. In principle, this should offer considerable advantages since most galaxies have detectable optical nebular line emissions. At the same time, these lines are easier to observe given their larger equivalent widths. Given the relative simplicity of these lines, measurements of velocities and velocity dispersions are straightforward.

The basic algorithm consists in calculating a model of the gravitational potential assuming that it is determined by the distribution of stars and an additional central mass. If the stars and the black hole mass dominate in such a way that the surrounding gas follow a Keplerian orbit, then the comparison between predictions and observations becomes simple. In particular, the mass of the black hole is a free parameter and must be varied in order to better fit the data. The best fit model will then give the best estimate of the central mass. Figure 2 shows the M84 example, where four different Keplerian fits have been over plotted to the data (black stars). The blue, green, red, and orange lines represent model predicitions assuming a black hole mass of 4.3, 4.5, 4.7 and 4.2 in units of $10^8 M_\odot$ respectively. As seen from the figure, a best fit is not clearly deduced, but we can infer that the mass should lie between $4.2 \times 10^8 M_\odot$ and $4.7 \times 10^8 M_\odot$ (Walsh et al. 2010).

Although the strengths of this model, there are many drawbacks that complicate its use. For instance, gas dynamics requires that gas must be distributed in radius to properly sample the

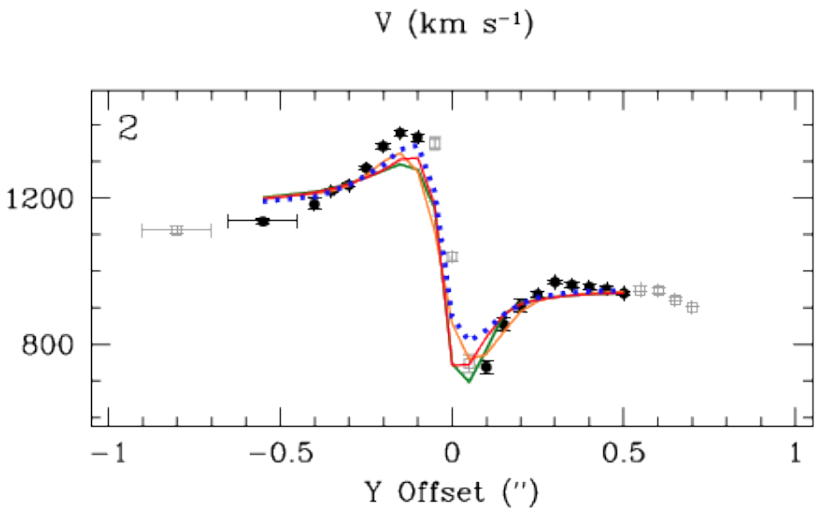

Fig. 2.— Example of black hole mass estimation using gas dynamics for M84. Black stars shows observational data, while blue, green, red, and orange lines show Keplerian fits assuming a black hole mass of 4.3, 4.5, 4.7 and 4.2 in units of $10^8 M_\odot$ respectively. A best fit for this model can not be extracted with certainty, but a range in which the black hole lies can be deduced. Adapted from Walsh et al. (2010)

radius of influence of the BH. In the same way, motion of gas needs to be ordered enough to be interpretable. Furthermore, one huge complication is that it assumes that gas dynamics are mostly influenced by gravitational forces from the interior mass. Unlike stars, gas might also be affected by other processes such as turbulence, shocks, and magnetic fields among others. In such a case, the observational data do not always show a Keplerian motion, and deviations from that profile might be observed. As a consequence, the fits do not give an accurate result and the mass of the black hole can not be estimated using this method.

2.3. Maser dynamics

Based on radio interferometry of water maser emission from cirum-BH molecular disks, maser dynamics have become a powerful tool to estimate BH masses. Analogously to the gas dynamics method, maser dynamics relies on measuring velocities from water megamasers orbiting in a torus surrounding the central black hole. The left panel in Figure 3 shows a representation of the torus and the location of masers in the galaxy NGC 4258. Maser dynamics follow two independent ways of measuring velocities. On one hand, it uses observations of nonsystemic-velocity components orbiting the BH in a Keplerian motion (blue and red dots in the figure). On the other hand, the near-systemic components allow us to measure the drift and the centripetal acceleration to calculate the central mass (green dots in the figure).

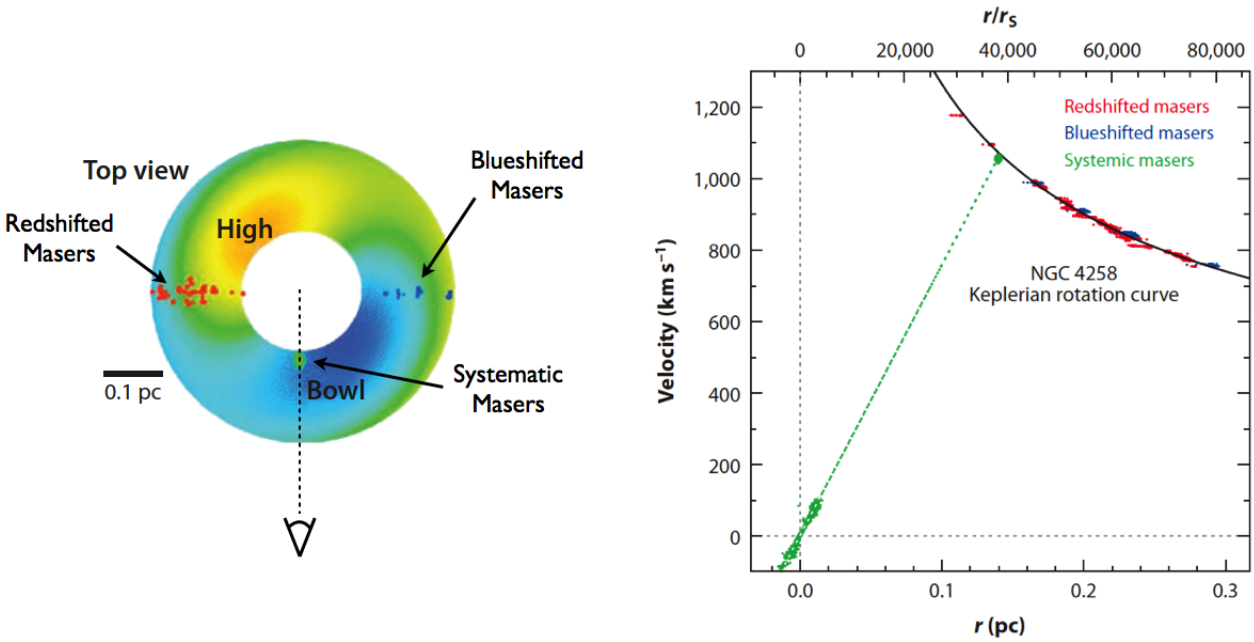

Fig. 3.— Example of maser dynamics for estimate black hole masses in the galaxy NGC 4258. On the left there is a diagram showing the torus surrounding the central object and the position of non-systemic (red and blue) and near-systemic masers (green). On the right, the same points are plotted in a velocity versus radius diagram. It is clearly seen that blue and red dots follow a Keplerian rotation curve. The green filled circle is the corresponding mean $V(r)$ point. Adapted from Kormendy & Ho (2013)

The right panel in Figure 3 illustrates these two methods. Non-systemic maser are shown in red and blue dots, corresponding to redshifted and blueshifted motions respectively. From the plot it is clear that those points follow a Keplerian rotation curve, which indicates that their motion is dominated by the BH and hence we can estimate its mass as $M_{\rm BH} = V^2 R/G$. Green dots show near-systemic masers, right in the line of sight between us and the central object. In this case we need measurements of the centripetal acceleration $V^2(r)/r$ and the linear velocity gradient along the line of sight. This last quantity can be easily converted to $V(r)/r$, which allows us to calculate the velocity as the ratio of both quantities. The latter method only requires the assumption that near-systemic masers are in circular motion around the center.

Although this method seems promising, it still has some disadvantages. A major complication is when the BH mass is not the dominant component of the gravitational field. That can happen when the mass of the disk enclosed by the masers is comparable to the mass of the central object, or in the presence of a massive nuclear star cluster. In those cases masers do not follow a Keplerian motion and deviations from this regime are observed. When those deviations are present in the rotation curves, we are not able to give an accurate estimation of the BH mass.

2.4. Reverberation mapping

This technique relies on the basic assumption that broad emission lines originate in a single central source close to the BH. In that case, the black hole mass can be easily calculated from the simple formula:

$$M_{\rm BH} = \frac{f \Delta V^2 R}{G} \tag{8}$$

where f is a coefficient accounting for the geometry of the problem, ΔV is the velocity width of the broad line region (BLR), R the size of the same region, and G the gravitational constant.

In order to measure the size of the BLR, we use emission lines from the BLR. It is believed that this emission arises from clouds that are excited by ionization radiation coming from the central source of energy. When this radiation changes its brightness, it will be reflected as variations ("reverberations") in the emission lines from the BLR. Given the finite velocity of the radiation, the inner regions of the BLR will show a variation before the outer parts of the same region. Obtaining that time difference, or delay, from observations and using the light speed, we can estimate the size of the BLR as $R = \tau c$ where τ is the lag and c the speed of light.

Now, using Equation 8 also requires measurements of the velocity width. But different parts of the emission line will give us different values for this parameter, hence the question is, what velocity should it be used? Estimations of the velocities usually follow two common approaches. The first option considers ΔV as the full width at half maximum (FWHM), while the second option simply uses the second moment of the line profile $\Delta V = \sigma_{\rm line}$. Hence, the measurement of velocities in the broad line emission constitutes one source of errors in the estimation of the BH mass.

But there is a more important factor in the formula that introduces uncertainties: f. The value of the virial coefficient f depends strongly on the geometry of the problem. For instance, a spherical distribution of clouds on random, isotropic orbits has $f = 3/4$ for $\Delta V =$ FWHM and $f = 3$ for $\Delta V = \sigma_{\rm line}$. A common practice to avoid this error is to calculate an average value for f for the sample of reverberation-mapped objects by requiring that they follow the same $M_{\rm BH} - \sigma$ relation as inactive galaxies. This reasonable, although unproven, assumption is motivated by the fact that reverberation-mapped AGNs with bulge stellar velocity dispersions measurements seem to follow an $M_{\rm BH} - \sigma$ relation.

3. $M_{\rm BH} - \sigma$ relation from observations

The idea of measuring this relation was suggested by Avi Loeb to two independent groups. The first results of the $M_{\rm BH} - \sigma$ relation were presented at the 2000 June AAS meeting in Rochester, and published later that year in the Astrophysical Journal Letters. For its most reliable sample, Ferrarese & Merritt (2000) (Figure 4, left panel) used 12 galaxies with BH masses measurements from absorption-line stellar spectra and motions of nuclear disks of gas and dust obtaining a slope

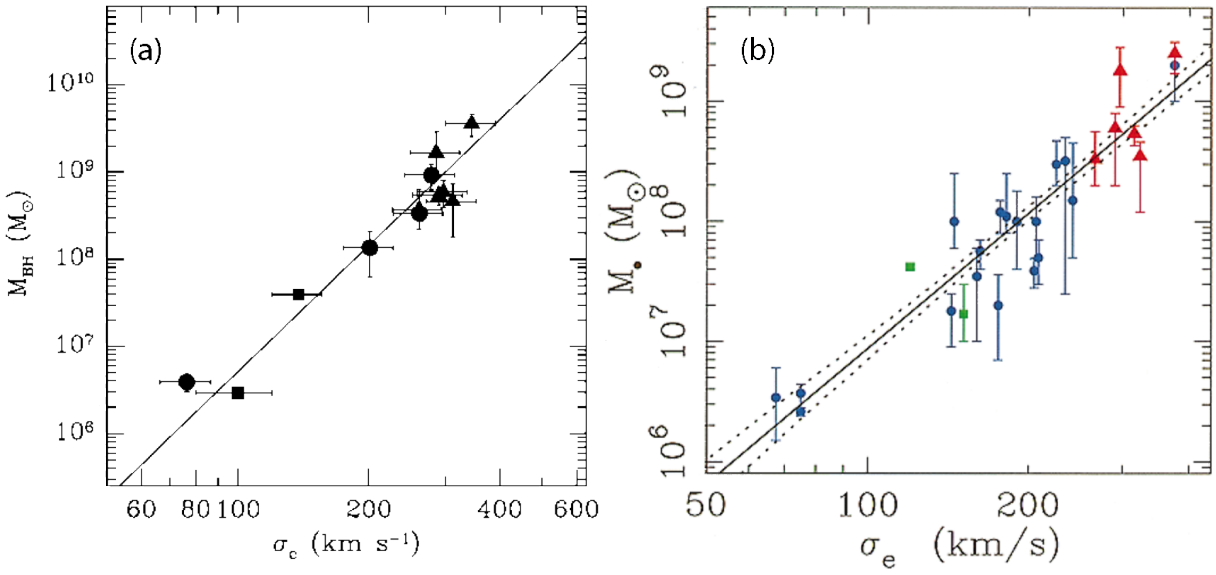

Fig. 4.— First measurement of the $M_{\rm BH} - \sigma$ relation. Panel (a) shows the data points and fit from Ferrarese & Merritt (2000), while panel (b) shows the results from Gebhardt et al. (2000). Both relations obtain a tight correlation between black hole masses and velocity dispersions of the host galaxy. A significant difference between them is the slope of the fit. While Ferrarese & Merritt (2000) quote $\beta = 4.8$, Gebhardt et al. (2000) deduce a value of 3.75.

of $\beta = 4.8$. Gebhardt et al. (2000) (Figure 4, right panel) doubles the sample, using a total of 26 galaxies with back hole measurements from masers, gas kinematics, and stellar kinematics with three-integrals models and obtaining a slope of 3.75.

Although both groups reported slopes that differ in more than three standard deviations, they agree in the low scatter present in the relation. Ferrarese & Merritt (2000) indicates that "most of this is due to observational errors", while Gebhardt et al. (2000) emphasizes "only 0.30 dex over almost 3 orders of magnitude in [$M_{\rm BH}$]". Many reasons have been proposed for explaining this. Among them, the most important one proposed by Tremaine et al. (2002) was that velocity dispersions were measured at different radii. Ferrarese & Merritt (2000) assumed the convention of measuring σ at $R_e/8$, which implied that some of their measurements had to be interpolated from values at greater radius. On the other side, Gebhardt et al. (2000) calculate velocity dispersions using a luminosity-weighted RMS line-of-sight dispersion within a slit aperture of half-length R_e.

Tremaine et al. (2002) further discuss that differences might be due to the different fitting methods used in both studies. On one hand, to find the parameters α and β of the fit in log-log space (Equation 1), Ferrarese & Merritt (2000) use the following formula:

$$\beta = \frac{\Sigma_{i=1}^{N}(y_i - \langle y \rangle)(x_i - \langle x \rangle)}{\Sigma_{i=1}^{N}(x_i - \langle x \rangle)^2 - \Sigma_{i=1}^{N}\epsilon_{xi}^2}, \qquad \alpha = \langle y \rangle - \beta \langle x \rangle$$

where $\langle x \rangle = N^{-1}\Sigma_{i=1}^{N} x_i$, and $\langle y \rangle = N^{-1}\Sigma_{i=1}^{N} y_i$. On the other hand, Gebhardt et al. (2000) compute the parameters minimizing χ^2 defined as:

$$\chi^2 = \sum_{i=1}^{N} \frac{(y_i - \alpha - \beta x_i)^2}{\epsilon_{yi}^2 + \beta \epsilon_{xi}^2}$$

Tremaine et al. (2002) argue that, although the second approach does not account for any intrinsic dispersion in the $M_{\rm BH} - \sigma$ relation, the fitting algorithm followed by Gebhardt et al. (2000) is a better choice. Among the disadvantages of the Ferrarese & Merritt (2000) method, the authors mention that errors in velocity dispersion might dominate for low-precision measurements, errors in black hole masses are not included, and that variables x and y are not treated symmetrically.

Ferrarese (2002) deepens more in the origin of these differences, and propose that only high-resolution measurements of BH masses should be included in the calculation of the slope. In particular, observations should resolve the radius of influence of the BH, i.e. $d_{\rm res}/R_{\rm infl} < 1$. The differences between high- and low- resolution observations were first studied in Ferrarese & Merritt (2000), obtaining slopes of 4.80 ± 0.54 and 5.81 ± 0.43 for the high- and low-resolution samples respectively. In a later study, Gültekin et al. (2009) rejected this argument arguing that a selection based on resolution might influence the sample, producing biased estimates of the intercept, slope, and intrinsic scatter of the relations. They suggest that this bias arises because $R_{\rm infl} \approx GM_{\rm BH}/\sigma^2$ and $M_{\rm BH} \approx \sigma^4$ so that $R_{\rm infl} \approx \sigma^2$. In that case, cuts defined by $R_{\rm infl}/d_{\rm res} > 1$ systematically exclude BH masses from the low-mass and low-velocity dispersion part of the $M_{\rm BH} - \sigma$ relation, which results in an overestimate of the intercept, an overestimate of the slope, and an incorrect estimate of the intrinsic scatter.

Since then, these differences have remained. Table 1 summarizes values for β obtained by studies ranging from 2000 until the most recent in 2013. Roughly speaking, values for the slope vary between 4 - 5, but more interesting than the slope is the fact that the scatter always remains very low. Although some papers have reported scatter as high as 0.44 dex (Gültekin et al. 2009), the trend is that it always remain comparable to error measurements. The tightness of the correlation gives powerful insights about a possible relation between the central black hole and its host galaxy.

The most recent study exploring this relation is Kormendy & Ho (2013) (Figure 5). In their study, they use a total of 48 data points, where BH masses have been derived using dynamical methods, including gas and stellar motions. It is worth noting that they have excluded BH masses based on kinematics of ionized gas when broad emission-line widths are not taken into account, arguing that they are usually underestimated. BH masses calculated in mergers in progress have also been excluded, based on the fact that they have abnormally small values. Finally, they did not include BH monsters in relatively small bulges and ellipticals. With all these considerations, they get a fit given by

$$\frac{M_{\rm BH}}{10^9 M_\odot} = (0.310^{+0.037}_{-0.033}) \left(\frac{\sigma}{200 \text{ km s}^{-1}} \right)^{4.38 \pm 0.29} \tag{9}$$

Reference	β	Scatter (dex)	Notes
Ferrarese & Merritt (2000)	4.8 ± 0.5	-	
Gebhardt et al (2000)	3.75 ± 0.3	0.30	
Merritt & Ferrarese (2001)	4.72 ± 0.36	-	
Ferrarese (2002)	4.58 ± 0.52	-	
Tremaine et al. (2002)	4.02 ± 0.32	0.25 - 0.3	
Ferrarese & Ford (2005)	4.86 ± 0.43	0.34	SMBHs with resolved $R_{\rm infl}$
Gultekin et al. (2009)	4.24 ± 0.41	0.44 ± 0.06	All galaxies
	3.96 ± 0.42	0.31 ± 0.06	Ellipticals
Kormendy & Ho (2013)	4.38 ± 0.29	0.29 ± 0.02	Classical bulges and Ellipticals

Table 1: Measurements of the $M_{\rm BH} - \sigma$ relation. From left to right, the columns indicates references, slope of the fit β, scatter of the relation, and additional notes. From these values it is clear that differences in the slope still exist, but the scatter keeps its low value.

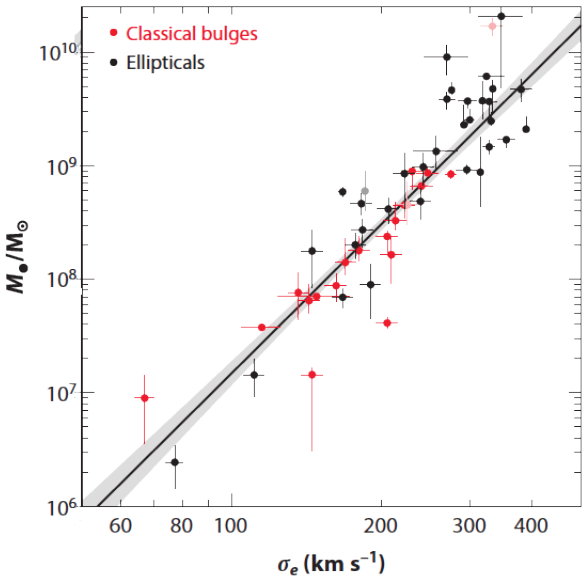

Fig. 5.— Most recent measurement of the $M_{\rm BH} - \sigma$ relation, from Kormendy & Ho (2013). In their sample they have only plotted elliptical galaxies and classical bulges, leaving out of the sample pseudobulges, disk galaxies and BH masses with anomalous behavior, such as on-going mergers and monster BHs in small bulges. Their best fit has a slope of $\beta = 4.38 \pm 0.29$ and a scatter of 0.29 ± 0.02. Figure from Kormendy & Ho (2013)

Kormendy & Ho (2013) go even further, and they argue that pseudobulges in disk galaxies do not follow the $M_{\rm BH} - \sigma$ relation. As seen previously, pseudobulges are believed to form from secular growth out of disk, while classical bulges are believed to be the result of major galaxy mergers. This determines that the characteristics of classical bulges are very similar to those of

elliptical galaxies, while pseudobulges are more disk-like structures. Figure 6 panel (a) shows the recent update of this relation by Kormendy & Ho (2013), where gray, red and blue dots account for elliptical galaxies, classical bulges, and pseudobulges, respectively. From the plot we can deduce that, although they do follow a weak relation, they lie systematically below the solid line, which is translated in an increment of the scatter in the fit. The same authors proposed this argument as one of the main reasons why previous studies have obtained dissimilar slopes, arguing that in those works there is no a clear differentiation between classical and pseudobulges.

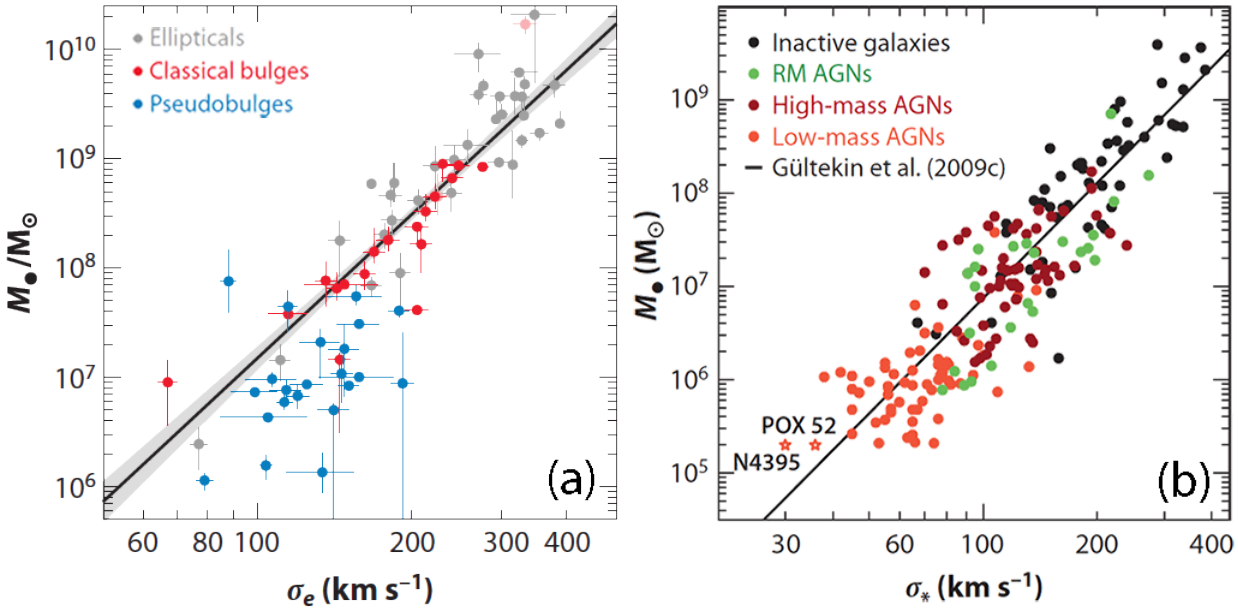

Fig. 6.— *Left:* $M_{\rm BH} - \sigma$ relation for elliptical galaxies (gray dots), classical bulges (red dots), and pseudobulges (blue dots). Pseudobulges lie systematically below the $M_{\rm BH} - \sigma$ relation, increasing its scatter when they are included. *Right:* $M_{\rm BH} - \sigma$ relation for active galactic nuclei, where σ is the stellar velocity dispersion. Active nuclei (green, dark red and orange dots) present a higher scatter than inactive galaxies (black dots). Adapted from Kormendy & Ho (2013)

At lower mass scales, observations have also shown that black holes in AGNs follow the $M_{\rm BH} - \sigma$ relation, with σ the stellar velocity dispersion (Peterson 2008). An updated version of this correlation is shown in Figure 6 panel (b), extracted from Kormendy & Ho (2013). The $M_{\rm BH} - \sigma$ relation is presented for reverberation mapping AGNs (green dots), high- (dark red dots), and low-mass AGNs (orange dots), in addition to inactive galaxies (black dots). The black hole masses are derived from reverberation mapping for green dots and spectroscopy of broad AGN emission lines for low- and high-mass AGNs. They found that a weak correlation is present down to $M_{\rm BH} \approx 10^5 M_\odot$ and $\sigma \approx 30$ km s^{-1} with significant higher scatter. They argue that uncertainties in the virial mass estimators extrapolated to low masses might dominate in that regime.

4. Other scaling relations

Given the apparent relation between black holes and its host galaxies, many others studies have tried to look for empirical relations between them. Two of the most important are the $M_{\rm BH} - L_{\rm bulge}$ and the $M_{\rm BH} - M_{\rm bulge}$ relations. The former was the first BH-host galaxy relation measured, and the precursor of the following studies of BHs-host galaxy coevolution. On the other hand, the $M_{\rm BH} - M_{\rm bulge}$ relation was explored based on the tightness of the $M_{\rm BH} - \sigma$ relation, and the relation between σ and $M_{\rm bulge}$ given by the virial theorem. In this section we will briefly describe both relations and compared them to the $M_{\rm BH} - \sigma$ relation.

4.1. Black hole Mass-Bulge Luminosity relation

The $M_{\rm BH} - L_{\rm bulge}$ relation was first proposed by Kormendy & Richstone (1995). Based on measurements of eight black hole masses, they pointed out that the estimated central black hole masses seemed to show a correlation with the host galaxy bulge luminosities following a power-law of the type $M_{\rm BH} \propto L_{\rm bulge}^{\gamma}$. They quoted a scatter of rms ~ 0.5 in $\log M_{\rm BH}$, which is greater compared to the scatter of the $M_{\rm BH} - \sigma$ fit. A later study by Magorrian et al. (1998) explored this relation in a sample of 32 nearby galaxies and their black hole masses, confirming that the estimated black hole mass in each galaxy was indeed proportional to the luminosity of the host galaxy bulge, with a scatter about the fit of approximately ± 0.5 dex. In a more recent study, Kormendy & Ho (2013) explore this relation with a refined sample, where only ellipticals and classical bulges are included (Figure 7 panel (a)). A difference with previous studies is that they consider luminosity in the K band in contrast to previous works that used luminosity in the B band, arguing that extinction is lower at those wavelengths and hence the K band is a better estimator of the luminosity of the galaxy. Their best fit model is given by

$$\frac{M_{\rm BH}}{10^9 M_\odot} = (0.544^{+0.067}_{-0.059}) \left(\frac{L_{K,\rm bulge}}{10^{11} L_{K\odot}} \right)^{1.22 \pm 0.08} \tag{10}$$

and a scatter of 0.30 ± 0.01. This value is as low as the scatter for the $M_{\rm BH} - \sigma$ relation showed in Equation 9. Previous studies have also found scatter values comparable, or even lower, to the $M_{\rm BH} - \sigma$ relation (Gültekin et al. 2009).

4.2. Black hole Mass-Bulge Mass relation

The $M_{\rm BH} - M_{\rm bulge}$ relation was first proposed by Marconi & Hunt (2003). They selected a sample of 37 galaxies with BH masses determined via direct gas kinematical or stellar dynamical determination. For the bulge mass, they assumed that the system was virialized, and hence they used the formula $M_{\rm bulge} = k R_e \sigma_e^2 / G$ to get the mass from velocity dispersions observations. In that case, the effective radius of the bulge, R_e, is extracted from observations. A factor of uncertainty

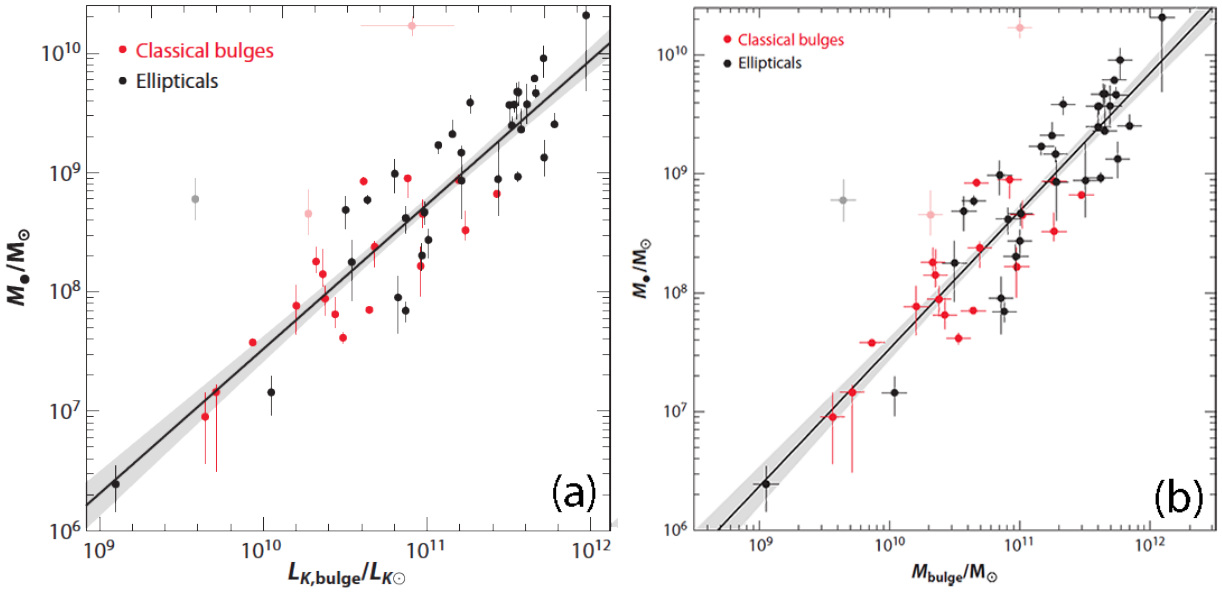

Fig. 7.— Most recent measurements for the $M_{\rm BH} - L_{\rm bulge}$ (panel (a)) and $M_{\rm BH} - M_{\rm bulge}$ (panel (b)) relations using the same points as in Figure 5. In the left plot, the best fit has the shape $M_{\rm BH} \propto L_{K,\rm bulge}^{1.22\pm0.08}$, while in the right plot the relation is of the form $M_{\rm BH} \propto M_{\rm bulge}^{1.17\pm0.08}$. In both relations the scatter is comparable to the scatter in the $M_{\rm BH} - \sigma$ relation. Adapted from Kormendy & Ho (2013).

is the constant k, which is strongly dependent on the geometry of the problem. For instance, if the bulge behaves as an isothermal sphere k takes the value of 8/3. To get a better estimation, the authors compare their $M_{\rm bulge}$ with $M_{\rm dyn}$ values obtained from dynamical modeling, and conclude that a value $k = 3$ gives a better correlation between both masses, so they adopt that value rather than 8/3. From their best fit, they obtained a relation consistent with $M_{\rm BH} \propto M_{\rm bulge}$. Kormendy & Ho (2013) updated this value using the same sample of galaxies than for the previous scaling relations (Figure 7 panel (b)). Their updated relation is given by

$$\frac{M_{\rm BH}}{10^9 M_\odot} = (0.49^{+0.06}_{-0.05}) \left(\frac{M_{\rm bulge}}{10^{11} M_\odot} \right)^{1.17\pm0.08} \tag{11}$$

with a scatter of 0.28, comparable to the scatter of both previous scaling relations.

4.3. A fundamental relation?

Although these relations have been proposed by different authors and at different times, they are not completely independent. We can connect them by taking into account other fundamental relations proposed in the literature. For instance, the Faber-Jackson relation (Faber & Jackson

1976) relates luminosity and velocity dispersion in elliptical galaxies. This gives us an additional expression of the form $L \propto \sigma^4$ which can be replaced in Equation 10. In such a case, from $M_{\rm BH} \propto L_{\rm bulge}^{1.22}$ we can obtain $M_{\rm BH} \propto \sigma^{4.88}$, which is close enough to the actual values derived from observations.

Analogously, the virial theorem gives us a relation of the form $M_{\rm bulge} \propto R_e \sigma_e^2$ where R_e can be obtained from observations. Hence, in viriliazed systems we can obtain a direct relation between the bulge mass and the velocity dispersion of the form $M_{\rm bulge} \propto \sigma_e^4$. Replacing this value in the $M_{\rm BH} - M_{\rm bulge}$ relation $M_{\rm BH} \propto M_{\rm bulge}^{1.17}$ we can recover the $M_{\rm BH} - \sigma$ relation.

Given these scaling relations and the interplay between them, now a new question arises: which one of these correlations is more fundamental? For many years a lower scatter has been measured in the $M_{\rm BH} - \sigma$ relation, which might be indicative of a more fundamental relation. But with new high-resolution observations and refined classification criteria, that hypothesis is not so clear anymore. Furthermore, finding a fundamental relation would give us some insights about the black hole-host galaxy relation, and their possible coevolution.

5. Conclusions

Since the first time they were observed, black holes have attracted a lot of attention. The launch of the Hubble Space Telescope in 1990 allowed us to get better understanding of its properties. In particular, it opened a whole new window for black hole demographics through high-resolution measurements of their masses, using methods such as stellar dynamics, gas dynamics, and masers dynamics. The combination of BH masses with observations of the properties of the host galaxy soon revealed a connection between these two components. First, Kormendy & Richstone (1995) found a correlation between BH masses and the bulge luminosity of the host galaxy. Five years later, Ferrarese & Merritt (2000) and Gebhardt et al. (2000) proposed a correlation between the mass of the central black hole, and the velocity dispersion of the host galaxy. Later on, in 2003, Marconi & Hunt (2003) suggestted a correlation between the BH mass and the mass of the bulge. Among those correlations, the $M_{\rm BH} - \sigma$ relation stood out because of its low scatter.

Since the seminal works of Ferrarese & Merritt (2000) and Gebhardt et al. (2000), the $M_{\rm BH} - \sigma$ relation has been studied for many authors. These works have the particular characteristic of not obtaining the same value of the slope for the fit. While Ferrarese & Merritt (2000) claims that $\beta = 4.8$, Gebhardt et al. (2000) quotes a slope of 3.75. Other studies have found values between 4 and 5, depending on the criteria to select BH masses. Many explanations have been proposed to account for dissimilarities in the slope. Among them we can find differences in the criteria to measure the velocity dispersion, dissimilar fitting models, and biased samples due to the resolution of the black hole mass measurements. Although this drawback and differences, most of them agree on reporting very low scatter, comparable to measurement errors. Recently, Kormendy & Ho (2013) updated those results, and proposed an $M_{\rm BH} - \sigma$ relation that holds for elliptical galaxies and classical bulges with a slope $\beta = 4.38$ and scatter 0.29 dex.

Other correlations, like the $M_{\rm BH}-L_{\rm bulge}$ and $M_{\rm BH}-M_{\rm bulge}$ relations have been studied through the years. Early measurements of these relations indicated a scatter larger than the one obtained for the $M_{\rm BH}-\sigma$ relation. Kormendy & Ho (2013) also updated these relations, and they found that both present a scatter comparable to the $M_{\rm BH}-\sigma$ relation. This arises a new question then: which relation is the tightest? Furthermore, if we consider that they are all related by the virial theorem, and the Faber-Jackson relation, then which one is the fundamental relation? Although we do not know the answer to this last interrogation, the message we get from observations is clear: There is a certain connection between black holes and their host galaxies.

Theories for explaining a correlation between the central black hole its host galaxy have abounded during the last decade, but none of them have successfully address this issue so far. Numerical simulations have suggested that galaxy merges generate inflows that feed gas to the central object and that the $M_{\rm BH}-\sigma$ is a consequence of this process (Di Matteo et al. 2005). Although this hypothesis has had a broad acceptance, it is still not a definite answer. Our best interpretation suggests that BHs and galaxies regulate each other's growth. Black hole may influence large scale galaxies by AGN feedback, while galaxies may influence BHs through feeding processes. Although these theories, we still lack of an understanding of the origin and implications of this relation. Furthermore, we do not know for sure the mechanisms involved in the coevolution of central black holes and host galaxies. These are still open questions, and further research is needed to clarify these issues.

REFERENCES

Di Matteo, T., Springel, V., & Hernquist, L. 2005, Nature, 433, 604

Faber, S. M., & Jackson, R. E. 1976, ApJ, 204, 668

Ferrarese, L. 2002, ApJ, 578, 90

Ferrarese, L., & Ford, H. 2005, Space Sci. Rev., 116, 523

Ferrarese, L., & Merritt, D. 2000, ApJ, 539, L9

Gebhardt, K., Bender, R., Bower, G., et al. 2000, ApJ, 539, L13

Genzel, R., Eisenhauer, F., & Gillessen, S. 2010, Reviews of Modern Physics, 82, 3121

Gültekin, K., Richstone, D. O., Gebhardt, K., et al. 2009, ApJ, 698, 198

Kormendy, J., & Ho, L. C. 2013, ARA&A, 51, 511

Kormendy, J., & Richstone, D. 1995, ARA&A, 33, 581

Magorrian, J., Tremaine, S., Richstone, D., et al. 1998, AJ, 115, 2285

Marconi, A., & Hunt, L. K. 2003, ApJ, 589, L21

Merritt, D., & Ferrarese, L. 2001, ApJ, 547, 140

Peterson, B. M. 2008, New A Rev., 52, 240

Sersic, J. L. 1968, Atlas de galaxias australes

Tremaine, S., Gebhardt, K., Bender, R., et al. 2002, ApJ, 574, 740

Walsh, J. L., Barth, A. J., & Sarzi, M. 2010, ApJ, 721, 762